# Initial Modeling of Urban Search Measurements

Douglas E. Peplow, Mathew W. Swinney, Gregory G. Davidson, Andrew D. Nicholson, Bruce W. Patton

*Oak Ridge National Laboratory, P.O. Box 2008, Oak Ridge, TN, 37831 peplowde@ornl.gov*

## INTRODUCTION

Detection of illicit nuclear materials in urban environments is difficult due to the large amount of background radiation from naturally occurring radioactive materials (NORM) in the roadways and buildings. Mobile searches suffer from low count rates, so the detection algorithms must be carefully balanced between missing real sources and reporting too many false alarms. The Modeling Urban Scenarios and Experiments (MUSE) project aims to create a virtual testbed for simulation of radiation detection to predict realistic background and threat source detection events so that detection algorithms can be better optimized to find illicit sources. The MUSE project is a collaboration of Oak Ridge National Laboratory (ORNL), Lawrence Berkeley National Laboratory (LBNL), and the Remote Sensing Laboratory (RSL). The project also works with staff at Lawrence Livermore National Laboratory (LLNL) to support the development of the Optimization Planning Tool for Urban Search (OPTUS) software package [1]. The first step in creating a virtual testbed is to determine the level of detail required in the models to match actual measurements.

Several measurement campaigns were conducted in 2015 and 2016 at the Fort Indiantown Gap (FTIG) Combined Arms Collective Training Facility (CACTF). This facility contains a representative urban environment, with a dozen buildings and several streets. Detectors commonly used in search operations—2 in × 4 in ×16 in NaI(Tl)—were used to measure count rates from background and sources [2]. Measurements with a shielded high-purity germanium detector of the roadways, sidewalks, and building walls were made to determine the concentration of NORM that makes up the bulk of the background radiation [3, 4].

This paper shows some comparisons of modeling simulations to measurements taken during the OPTUS-3 campaign in November 2015. Measurements with and without an 81 μCi cesium source were made at several points along the center line of the main road. Initial results show good agreement between the measured and simulated spectra above 300 keV. Additional studies to determine the causes of mismatch below 300 keV have been started and will also be discussed.

## MEASUREMENTS

Four source locations were used, with several detector locations for each source location. For some combinations of source and detector positions, there was a direct line of sight between the two. In other cases, the direct line of sight was blocked by buildings. Distances between the source and detector varied between 12 and 35 meters. The source and detector locations are listed in Table 1 and shown in Fig. 1. Seven background measurements were taken, and 19 measurements with the cesium source were also taken. Measurement locations are denoted using the distance from the center of the left intersection. The detectors were oriented with the 4 in × 16 in faces toward the buildings and the long axis aligned with the roadway.

Table I. Source and Detector Locations

| Source | Distance from road centerline (m) | Road centerline detector locations (m) |
|---|---|---|
| 1 | 16.5 | 10, **20**, **30**, **40**, 50 |
| 2 | 30.0 | 10, 20, **30**, 40 |
| 3 | 11.0 | **30**, **40**, 50, 70, **80** |
| 4 | 16.5 | **30**, **40**, **50**, **70**, 80 |

Note: direct line-of-sight locations in **bold**; locations with no data recorded in red


Fig. 1. Overhead view of FTIG CACTF main street
- source locations 1–4
- detector locations10–80
- asphalt (gray)
- gravel (light gray)
- concrete intersections (white)

## MODEL

A 3D computational model of the FTIG CACTF for use in the SCALE/MAVRIC [5] radiation transport package was developed from the construction drawings supplied by the US National Guard. The current model focuses on the area near the main street and includes four concrete intersections, six asphalt roads, a gravel road, sidewalks,

curbs, soil with a rough approximation of terrain elevation, and nine buildings. Eight of the buildings consist mostly of just their outer shells, but the three-story hotel includes interior floors and walls since measurements have been made inside that building during previous campaigns. The size of the model (Fig. 2), is 416 ft × 409 ft × 66.667 ft (126.8 m × 124.7 m × 20.3 m). Materials in the model were assigned based on information in construction drawings. Elemental composition and density for each material were taken from standard materials definitions for transport [6].

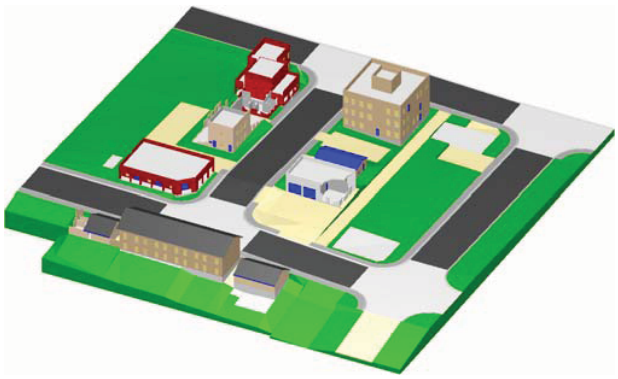

Fig. 2. FTIG CACTF model with nine buildings
concrete intersections (white)
asphalt (black)
gravel (cream)
soil (green)

For photon detectors in urban areas, nearly all of the background is due to the presence of NORM in the soil, roadways, and buildings. The main contributors to NORM are $^{40}$K, $^{232}$Th and its daughter products, and $^{238}$U/$^{235}$U and their daughters. In order to model the background at the FTIG CACTF site, sources were defined in roads, sidewalks, curbs, soil, and buildings using the NORM concentration values determined from the HPGe measurements [3]. The energy spectra for the NORM components were computed using SCALE/ORIGEN [5] to accurately account for all daughter products. The calculation assumed that the daughter products were all in transient equilibrium with the parent, which may not always be the case. Radon is present in the thorium and uranium decay sequences, and because it is a noble gas, it could escape from the material before it decays into the next isotope in the decay sequence. Materials processing techniques could also alter the elemental ratios by preferentially removing elements midway in the decay chains (called *technologically enhanced* NORM, or TENORM). In the process of determining the NORM concentration values for the FTIG CACTF materials [3, 4], the concentrations of several individual isotopes in each decay chain were determined and were consistent with the transient equilibrium assumption.

Typically, radiation transport codes require the user to define the geometric extent and strength of each source. The volume of the source is required to determine the strength. Because the materials with NORM sources have very large extents with difficult-to-compute volumes (soil) or consist of a large number of small bodies (cinder block walls of buildings), a more automated approach was taken in constructing source descriptions. A 416 × 409 × 66 mesh (1ft$^3$ voxels) was overlaid across the geometry model and the fraction of each real material within each voxel was determined. With these values, the total volume of each material across the site could be found and the total strength determined. A set of mesh-based sources, one for each material/NORM component combination, was created. Biasing factors were applied to each of the mesh-based sources so that when they were used in a Monte Carlo calculation, more photons would be sampled nearest the centerline of the main street.

A common way to efficiently simulate detector systems is to break the simulation into two steps: (1) transport photons from the various sources to determine the energy-dependent flux at the detector locations, and (2) transport photons within the detector to compute the energy deposited pulse height distribution, which is the basis of the final spectrum. Note that the detectors are not modeled in the first step, so the same transport calculation for step 1 can be used with several different types of detectors in step 2. The calculations in step 2 can be performed once for each type of detector of interest: each calculation is called a *detector response function*. After running step 1, the energy-dependent fluxes from anywhere in the transport model can be folded with one or more detector response functions, which is much more efficient than explicitly modeling individual detectors in a site-wide transport calculation.

For this project, three detector response functions were created for a 2 in × 4 in × 16 in NaI(Tl) crystal surrounded by 1 mm of aluminum using MCNP [7]. Photons incident perpendicularly to the 2 in × 4 in face (orientation 1), the 2 in × 16 in face (orientation 2) and the 4 in × 16 in face (orientation 3) were considered. In each orientation, for a given monoenergetic unit flux (photons/cm$^2$/s), the pulse height distribution (counts/s) was determined. A short utility code was written to take an energy-dependent flux and apply one of the three response functions to determine the total pulse height distribution. The expectation is that the real detector response would be a weighted combination of the computed responses for orientations 2 and 3: incident photons mainly enter these two faces of the detector. Photons from the road underneath enter face 2, and photons from far away or from buildings enter face 3. Real detectors also have an energy-dependent resolution that broadens the peaks of the pulse height spectrum. To account for this, another utility program was created to apply a simple energy resolution function similar to what GADRAS [8] uses for NaI(Tl) detectors.

## COMPARISON OF RESULTS

The MAVRIC Monte Carlo background calculation used weight windows in addition to the biased sources to reduce the variance of the energy dependent flux along the main street. Fluxes were processed with the response functions for orientations 2 and 3. The Monte Carlo run time required about 1,500 hours to reduce the channel-by-channel statistical uncertainties to minimize the impact the final detector spectra.

Figure 3 shows the measured background and simulations (using two detector response functions) for the detector position at 30 m. Agreement is good over a large energy range. Predicted values are a bit high at the $^{40}$K peak (1461 keV) and are low below 300 keV. These mismatches were observed for all seven of the detector locations.

MAVRIC was run for 40 hours for each of the four source locations, with the runtime set long enough so that statistical uncertainties did not impact the final spectrum. Only the 81 μCi of cesium source was included in the simulations. The NORM background from above was added to the cesium source results to produce the total predicted spectrum. An example from source location 1 and detector location at 30 m is shown in Fig. 4 for the energy region near the cesium 662 keV line. This peak overlaps with the $^{214}$Bi 609 keV peak. The same data are shown in Fig. 5, comparing just the cesium source response to the background-subtracted measured values. In this case, orientation 3 should match well because most photons from the source enter face 3. The full spectra for the background-subtracted comparison is shown in Fig. 6 using broader energy bins for the measured data to reduce the statistical noise. For source locations 1, 2, and 4, the background-subtracted measured values lie between predictions of the two orientations. For source location 3, both orientations are higher than the background-subtracted measured values.

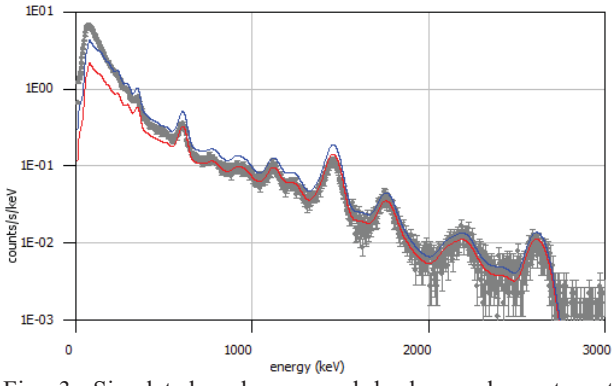


Fig. 3. Simulated and measured background spectra at detector location at 30 m. Measurements (gray) include the 1-σ uncertainties, and simulated results show two detector responses: 2 in × 16 in face (red) and 4 in × 16 in face (blue).

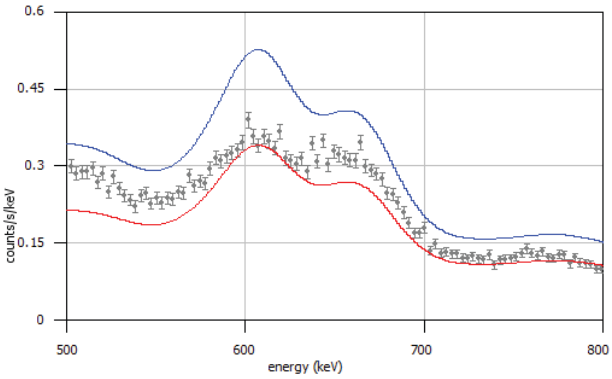


Fig. 4. Peak area comparison of measured values (gray) and simulated detector responses, 2 in × 16 in face (red) and 4 in × 16 in face (blue), for source location 1 and detector location at 30 m.

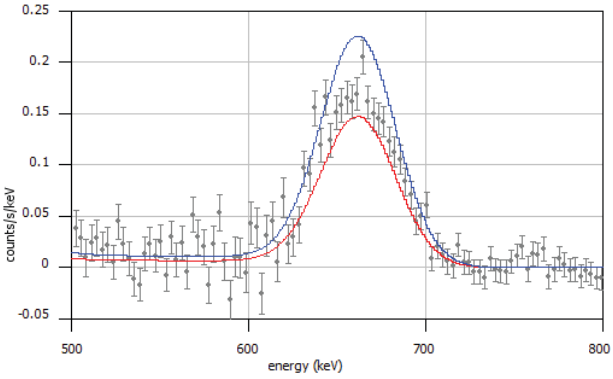


Fig. 5. Peak area comparison of background-subtracted measured values (gray) and simulated detector responses, 2"×16" face (red) and 4"×16" face (blue), for source location 1 and detector location at 30 m.

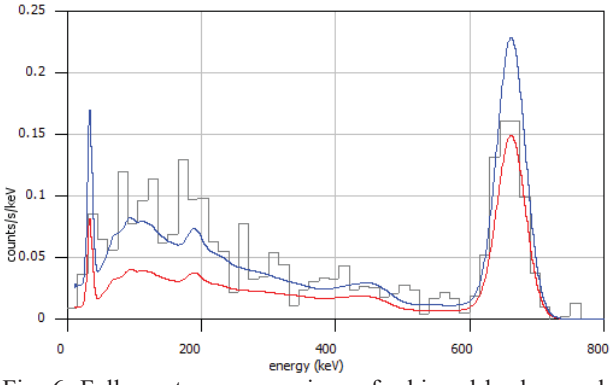


Fig. 6. Full spectrum comparison of rebinned background-subtracted measured values (gray) and simulated detector responses, 2 in × 16 in face (red) and 4 in × 16 in face (blue), for source location 1 and detector location at 30 m.

## ADDITONAL STUDIES

For the background simulations, two items are being explored to explain/improve the agreement between measurements and predictions in the low-energy region of the spectrum. First, the lack of skyshine from more distant background sources is being studied. Second, the lack of scattering material near the detector—such as the table holding the detector and the associated electronics next to the detector—is being examined. Both of these additions are expected to increase the response at low energy.

Initial skyshine studies that added increasingly larger amounts of soil and air to a simple model of a detector 1 meter above a ground indicated that about 500 m of ground in each direction and 500 m of air were required before the simulated spectra stopped increasing. Preliminary calculations using extra soil and extra air around the FTIG model show about a factor of two increase in the final background spectrum in the low-energy region.

Adding materials around the detector location also increases the low-energy portion of the predicted spectrum (only 5–15%) due to photons scattering into the detector that otherwise would have missed the detector. There is also a slight (~2%) decrease in the high-energy portion of the spectra, as photons are scattered or absorbed by the materials close to the detector.

Both of these items, as well as other items such as radon daughters in the air, need to be examined more fully to determine what is required for background simulations to match measurements. An improved detector response function is also being developed to better account for the angular flux at the detector location.

## SUMMARY

Initial Monte Carlo simulations of measurements conducted at the FTIG CACTF using detailed models and measured NORM concentrations agree with the measured spectra quite reasonably. Under-prediction in the low-energy portion of the spectrum may be remedied by the inclusion of larger extents of ground, larger extents of air, and materials near the detector (possibly within the detector response function).

Even with the low-energy under prediction, synthetic detector event data derived from Monte Carlo simulations show enough representative detail that they will be used as the basis of a detection algorithm competition. Data sets with and without sources will be prepared for virtual city streets and then given to competitors to test their detection algorithms against.

## ACKNOWLEDGMENTS

This work was sponsored by the Enabling Capabilities for Nonproliferation and Arms Control (EC) Program Area (James J. Peltz and Donald E. Hornback, Program Managers) of the Office of Defense Nuclear Nonproliferation Research and Development, National Nuclear Security Administration. The authors would like to thank M. S. Lance, K. McLean, Alexander A. Plionis, and their team of technicians from RSL who collected the data at FTIG.

## REFERENCES

1. R. WHEELER, D. FAISSOL, C. SANTIAGO, T. BAGINSKI, and K. NELSON, "Physics and Optimal Routing for Urban Radiation Source Search," 2016 IEEE International Conference on Multisensor Fusion and Integration for Intelligent Systems, Special Session on Multisensor Fusion Methods for Radiation Source Localization, Baden-Baden, Germany (September 19–21, 2016).

2. A. D. NICHOLSON, I. GARISHVILI, D. E. PEPLOW, D. E. ARCHER, W. R. RAY, M. W. SWINNEY, G. G. DAVIDSON, S. L. CLEVELAND, B. W. PATTON, D. E. HORNBACK, J. J. PELTZ, M. S. L. MCLEAN, A. A. PLIONIS, B. J. QUITER, and M. S. BANDSTRA, "Multi-Agency Urban Search Experiment Detector and Algorithm Test Bed," submitted to *IEEE Transactions on Nuclear Science* (2016).

3. M. W. SWINNEY, D. E. PEPLOW, A. D. NICHOLSON, and B. W. PATTON, "NORM Concentration Determination in Common Construction Materials in an Urban Environment," *Transactions of the American Nuclear Society* **114**, 635–638 (2016).

4. M. W. SWINNEY, D. E. PEPLOW, and A. D. NICHOLSON, "Characterization of NORM in an Urban Environment using HPGe Measurements and MCNP6 Simulations," submitted to *Transactions of the American Nuclear Society* **116** (2017).

5. *SCALE: A Comprehensive Modeling and Simulation Suite for Nuclear Safety Analysis and Design*, ORNL/TM-2005/39, Version 6.1 (2011). Available from Radiation Safety Information Computational Center at Oak Ridge National Laboratory as CCC-785.

6. R. J. McCONN, JR., C. J. GESH, R. T. PAGH, R. A. RUCKER, and R. G. WILLIAMS III, "Compendium of Material Composition Data for Radiation Transport Modeling," PNNL-15870, Rev. 1, Pacific Northwest National Laboratory, Richland, Washington, March 2011.

7. T. GOORLEY, et al., "Initial MCNP6 Release Overview," *Nuclear Technology* **180**, 298–315 (2012); http://dx.doi.org/10.13182/NT11-135.

8. D. J. MITCHELL, L. T. HARDING, G. G. THORESON, and S. M. HORNE, "GADRAS Detector Response Function," SAND2014-1946, Sandia National Laboratories, Albuquerque, New Mexico, November 2014.